Title	Urinary chemokine (C-C motif) ligand 2 (monocyte chemotactic protein-1) as a tubular injury marker for early detection of cisplatin-induced nephrotoxicity.
Author(s)	Nishihara, Kumiko; Masuda, Satohiro; Shinke, Haruka; Ozawa, Aiko; Ichimura, Takaharu; Yonezawa, Atsushi; Nakagawa, Shunsaku; Inui, Ken-Ichi; Bonventre, Joseph V; Matsubara, Kazuo
Citation	Biochemical pharmacology (2013), 85(4): 570-582
Issue Date	2013-02-15
URL	http://hdl.handle.net/2433/169686
Right	© 2012 Elsevier Inc.
Type	Journal Article
Textversion	author

Title

Urinary chemokine (C-C motif) ligand 2 (monocyte chemotactic protein-1) as a tubular injury marker for early detection of cisplatin-induced nephrotoxicity

Authors

Kumiko Nishihara, Satohiro Masuda, Haruka Shinke, Aiko Ozawa, Takaharu Ichimura, Atsushi Yonezawa, Shunsaku Nakagawa, Ken-ichi Inui, Joseph V. Bonventre, Kazuo Matsubara

Affiliations

Department of Pharmacy, Kyoto University Hospital, Faculty of Medicine, Sakyo-ku, Kyoto 606-8507, Japan (K.N., S.M., H.S., A.O., A.Y., S.N., K.I., K.M.)
Renal Division, Brigham and Women's Hospital, Harvard Medical School, Harvard Institutes of Medicine, Room 576, 4 Blackfan Circle, Boston, MA 02115, USA (T.I., J.B.)
Present address of K.I.: Kyoto Pharmaceutical University, Yamashina-ku, Kyoto 607-8414, Japan.

Correspondence to   Satohiro Masuda, Ph.D.

Department of Pharmacy

Kyoto University Hospital

Sakyo-ku, Kyoto 606-8507, Japan

TEL.: +81-75-751-3586

FAX: +81-75-751-3586

E-mail: masuda@kuhp.kyoto-u.ac.jp

Classification

Pulmonary, Renal and Hepatic Pharmacology

Abstract (250 words)

Because of the difficulty in detecting segment-specific response in the kidney, we investigated the molecular events underlying acute kidney injury in the proximal tubules of rats with cisplatin (cis-diamminedichloroplatinum II)-induced nephrotoxicity. Microarray analysis revealed that mRNA levels of several cytokines and chemokines, such as interleukin-1beta, chemokine (C-C motif) ligand (CCL) 2, CCL20, chemokine (C-X-C motif) ligand (CXCL) 1, and CXCL10 were significantly increased after cisplatin treatment in both isolated proximal tubules and whole kidney. Interestingly, tubular CCL2 mRNA levels increased soon after cisplatin administration, whereas CCL2 mRNA levels in whole kidney first decreased and then increased. Levels of both CCL2 and kidney injury molecule-1 (KIM-1) in the whole kidney increased after cisplatin administration. Immunofluorescence analysis revealed CCL2 changes in the proximal tubular cells initially and then in the medullary interstitium. Urinary CCL2 excretion significantly increased approximately 3-fold compared with controls the day after cisplatin administration (5 mg/kg), when no changes were observed plasma creatinine and blood urea nitrogen levels. Urinary levels of KIM-1 also increased 3-fold after cisplatin administration. In addition, urinary CCL2 rather than KIM-1 increased in chronic renal failure rats after administration of low-dose cisplatin (2 mg/kg), suggesting that urinary CCL2 was selective for cisplatin-induced nephrotoxicity in renal impairment. These results indicated that the increase in cytokine and chemokine expression in renal epithelial cells might be responsible for kidney deterioration in cisplatin-induced nephrotoxicity, and that urinary CCL2 is associated with tubular injury and serves as a sensitive and noninvasive marker for the early detection of cisplatin-induced tubular injury.

1. Introduction

Avoiding renal injury is important in routine medical treatment because many nephrotoxic drugs can lead to tubular damage and result in acute kidney dysfunction [1]. Nephrotoxicity resulting from drug exposure has been estimated to contribute to 19–25% of all cases of acute kidney injury in critically ill patients [2]. Ionic drugs are mainly secreted by tubular organic ion transporters across the luminal membranes of renal tubular epithelial cells after uptake from the blood by transporters in the basolateral membranes of the proximal tubules [3]. In addition, filtered and secreted toxins can be concentrated within the lumen of the tubule as fluid is reabsorbed. Therefore, proximal tubules are extraordinarily susceptible to drug-induced nephrotoxicity. The kidney is structurally complicated, consisting of many segments and cell types. Thus, it is difficult to investigate molecular events specific to a single nephron segment.

Cisplatin (cis-diamminedichloroplatinum II) is one of the most effective chemotherapeutic agents against solid tumors, including testicular, head and neck, ovarian, and non-small cell lung cancers [4]. Despite its strong anti-tumor effects, severe nephrotoxicity limits clinical use. A basolateral organic cation transporter, OCT2 (SLC22A2), mediates cisplatin transport from the circulation into proximal tubular epithelial cells, and renal proximal tubules are widely acknowledged to be major targets of cisplatin-induced nephropathy [5, 6]. Although several therapeutic strategies have been suggested for preventing cisplatin-induced renal injury, no effective treatments have been found aside from vigorous hydration [7]. In addition, a mechanism-based marker for detecting early cisplatin-induced proximal tubule injury has not been clinically developed. Creatinine and blood urea nitrogen levels increase significantly

only after substantial kidney injury occurs, and then after a significant time delay. Thus, monitoring the early responses of the proximal tubules to prevent further decline in renal function is important.

We hypothesized that evaluating proximal tubule–specific changes would clarify the molecular mechanisms underlying cisplatin-induced nephrotoxicity and could lead to new markers for the detection of proximal tubule–specific injury. In the present study, we used microarray analyses of isolated proximal tubules. In addition to evaluating gene expression in the kidneys of rats with cisplatin-induced nephropathy, we measured urinary levels of chemokine (C-C motif) ligand (CCL) 2 (also known as monocyte chemotactic protein-1, MCP-1) and kidney injury molecule-1 (KIM-1) for potential use as markers for the early detection of cisplatin-induced nephropathy.

2. Materials and Methods

2.1. Animals

Male Wistar/ST rats (8 weeks old) were purchased from SLC Animal Research Laboratories (Shizuoka, Japan). The rats were provided with a standard pelleted food and water ad libitum. Cisplatin (0.5 mg/mL; Randa®; Nippon Kayaku Co. Ltd., Tokyo, Japan) was administered intraperitoneally; the same volume of saline solution was injected into the sham controls. For microarray analysis, rats treated with 2 and 10 mg/kg cisplatin 2 days after administration were used. For real-time PCR, immunofluorescence analysis, and measurements of urinary biomarkers, rats treated with 5 mg/kg cisplatin were used the next day, as well as 2, 4 and 7 days after administration, since more than half of the rats treated with 10 mg/kg of cisplatin died by the 4th day. Rats treated with the same volume of saline were used as Sham-treated rats. For the chronic renal failure model, cisplatin (2 mg/kg) or saline (vehicle) was administered on the 14th day after subtotal nephrectomy [8], and urine and blood samples were collected on days 1, 2, 4, and 7 after the administration of cisplatin or vehicle. Rats were maintained in metabolic cages for 24 h to determine urinary output levels and creatinine clearance. At time 0 and each day after cisplatin administration, plasma, bladder urine, and kidneys were collected. All the protocols were approved by the Animal Research Committee, Graduate School of Medicine, Kyoto University.

2.2. Functional and histological examination of the kidneys

Creatinine, blood urea nitrogen, and urinary albumin levels and the enzymatic activity of *N*-acetyl-β-D-glucosaminidase in bladder urine were measured as previously described [9]. For histological examination, kidneys were fixed in ethyl Carnoy's

solution and stained with periodic acid-Schiff reagent (Sapporo General Pathology

Laboratory Co. Ltd., Hokkaido, Japan).

2.3. Isolation of renal proximal tubules via microdissection

Microdissection was performed as previously reported [8, 10]. Briefly, rats were

anesthetized with sodium pentobarbital (50 mg/kg intraperitoneally). The abdominal

aorta was ligated just above and just below the left renal artery. The left kidney was

perfused with 10 mL solution A (130 mM NaCl, 5 mM KCl, 1 mM NaH_2PO_4, 1 mM

$MgSO_4$, 1 mM calcium lactate, 2 mM sodium acetate, 5.5 mM D-glucose, and 10 mM

N-2-hydroxyethylpiperazine-*N′*-2-ethanesulfonic acid, pH 7.4) through the abdominal

aorta and then with 10 mL solution B. Solution B consisted of solution A with 1 mg/mL

collagenase A (Roche Diagnostic GmbH, Mannheim, Germany), 1 mg/mL bovine serum

albumin (Sigma-Aldrich, St. Louis, MA, USA), and 10 mM vanadyl ribonucleotide

complex (VRC; New England BioLabs Inc., Ipswich, MA, USA).

Kidney slices were cut along the corticomedullary axis and incubated in solution B

for 30 min at 37°C under aeration with 100% O_2. After a wash with ice-cold solution A,

the samples were microdissected with needles under a stereomicroscope at 10°C in

solution A1 (solution A containing 10 mM vanadyl ribonucleotide complex) to obtain

proximal tubules from the superficial nephron. Twenty millimeters of each proximal

tubule was used for total RNA extraction. Total RNA was extracted with an RNeasy

Mini Kit (Qiagen GmbH, Hilden, Germany), concentrated through ethanol precipitation,

and used for microarray or real-time polymerase chain reaction (PCR) analysis.

2.4. Gene expression array system

Digoxigenin-labeled cRNA was generated from total RNA extracted from the

proximal tubules or whole kidney using a chemiluminescent reverse transcription-*in*

vitro transcription labeling kit (v2.0; Applied Biosystems, Foster City, CA, USA). Ten

micrograms of labeled cRNA from each reverse transcription reaction was hybridized

onto a Rat Genome Survey Microarray (Applied Biosystems) at 55°C for 16 h following

manufacturer recommendations. Microarrays were analyzed using an ABI 1700

Chemiluminescent Microarray Analyzer (Applied Biosystems).

2.5. Gene expression data analysis

The array contained 34,656 oligonucleotide probes, including 26,857 individual

gene probes and more than 1000 control probes. Microarray signal data were analyzed

using Spotfire® (TIBCO Software Inc. Palo Alto, CA). Expression values were

normalized across the experiments with 50% percentile values from each experiment.

Genes were defined as detectable based on recommendations from Applied Biosystems:

a gene with a signal-to-noise ratio of >3.0 in 2 or 3 assays and a FLAG value of <5000

was considered detectable. Normalized signal data were analyzed statistically with

1-way analysis of variance. Probability (P) values of <0.05 were considered statistically

significant. The microarray data were deposited in the National Center for

Biotechnology Information Gene Expression Omnibus

(http://www.ncbi.nlm.nih.gov/geo/) and are accessible through accession number

GSE37133.

2.6. Real time-PCR analysis using isolated proximal tubules and whole kidney

Total rat kidney RNA was extracted using a MagNA Pure LC RNA Isolation

Kit-High Performance (Roche Diagnostic GmbH) according to manufacturer

instructions. Total RNA from renal proximal tubules was isolated as described above.

RNA was reverse-transcribed with random hexamers using Superscript II reverse

transcriptase (Invitrogen part of Life Technologies Corp., Carlsbad, CA, USA) and

digested with RNase H (Invitrogen). Real-time PCR was carried out with an ABI

PRISM 7700 Sequence Detector (Applied Biosystems) according to manufacturer

instructions in a total volume of 20 µL containing 5 µL reverse-transcribed cDNA, 1

µM forward and reverse primers, 0.2 µM TaqMan probe, and 10 µL TaqMan Universal

PCR Master Mix (Applied Biosystems). Glyceraldehyde-3-phosphate dehydrogenase

mRNA expression was measured as an internal control. mRNA quantification was

performed as reported elsewhere [8].

2.7. Immunofluorescence analysis

Animals were anesthetized and their kidneys were perfused through the abdominal

aorta, first with saline containing 50 U/mL heparin and then with 4% paraformaldehyde

in phosphate-buffered saline (PBS). Fixed tissues were embedded in Tissue-Tek[®] OCT

compound (Sakura Finetechnical, Tokyo, Japan) and frozen rapidly in liquid nitrogen.

Sections (5 µm thick) were cut, permeabilized with 0.3% Triton X-100 in PBS for 30

min, and incubated at 37°C for 60 min covered with goat serum (Wako, Osaka, Japan)

for detecting CCL2 or with 5% bovine serum albumin in PBS containing 0.3% Triton

X-100 for detecting Kim-1, interleukin (IL)-1beta, CCL20, chemokine (C-X-C motif)

ligand (CXCL) 1, and CXCL10. The covered sections were incubated with antisera

specific for CCL2, CXCL10 (Santa Cruz Biotechnology, Santa Cruz, CA, USA),

IL-1beta (R&D Systems Inc., Minneapolis, MN, USA), CCL20 (Abcam, Cambridge, UK), CXCL1 (LifeSpan Biosciences Inc., Seattle, WA, USA), or Kim-1 at 4°C overnight [9, 11]. After further washing with PBS, the sections were incubated with Alexa Fluor 546-labelled second antibody (Invitrogen), Alexa Fluor 488-labeled phalloidin (Invitrogen), and 4′,6-diamidino-2-phenylindole (Wako) at 37°C for 60 min. The sections were examined, and images were captured with a BZ-9000 (Keyence, Osaka, Japan).

2.8. *Measuring urinary, plasma, and kidney CCL2 and urinary KIM-1 levels*

An additional experiment was performed to obtain urine samples from rats treated with 5 mg/kg cisplatin [12]. Urine samples were collected directly from the bladder when the kidneys were harvested. Protease inhibitor cocktail (Nacalai Tesque Inc., Kyoto, Japan) and phosSTOP (Roche Diagnostic GmbH) were added, and the urine and kidney tissue was stored at –80°C. The lysate of kidney samples was prepared as described in another report [13]. Concentrations of urinary and plasma and kidney lysate CCL2 were measured using an enzyme-linked immunosorbent assay kit (rat MCP-1; Immuno-Biological Laboratories Co. Ltd., Gunma, Japan). CCL2 concentrations were normalized to urinary creatinine concentration. Urinary and kidney lysate KIM-1 protein levels were measured using microsphere-based Luminex xMAP technology developed in the Vaidya/Bonventre laboratories as described previously [14, 15].

For the chronic renal failure model, 6-week-old rats were subtotally nephrectomized as described elsewhere [8, 9, 11]. In brief, the right kidney was removed, and the posterior and anterior apical segmental branches of the left renal artery were

individually ligated. Previously, we have reported that the plasma level of testosterone decreased after nephrectomy, and the renal expression level of OCT2 was markedly decreased with decreased renal distribution of cisplatin [5]. Therefore, testosterone enanthate (2.5 mg/mL corn oil) was subcutaneously administered to nephrectomised rats at a dose of 200 μL/body (0.5 mg/body) on the day of nephrectomy and on days 3, 8, and 13 after nephrectomy to maintain the expression level of OCT2 and renal uptake of cisplatin [16].

2.9. Statistical analyses

Data are expressed as mean ± standard error. Data were analyzed statistically using the unpaired Student *t* test. Multiple comparisons were performed with Dunnett's 2-tailed test after 1-way analysis of variance. P values of <0.05 were considered statistically significant.

3. Results

3.1. Comparison of gene expression profiles in isolated proximal tubules and whole kidneys

Microarray analyses were carried out using total RNA samples isolated from microdissected proximal tubules and whole kidney. Of the 26,857 gene probes, 12,840 and 10,915 were detected in the isolated proximal tubules and whole kidney, respectively. Of these, 8,206 genes were expressed in both tissue. We analyzed the expression of solute carrier (Slc) family genes to evaluate the specificity of the microarray assay in isolated tubules. Slc family genes are abundantly expressed in renal proximal tubules, and their distribution pattern across kidney segments has been determined. As shown in Table 1, expression levels of 23 of the 184 Slc genes differed by at least 5-fold between isolated tubules and whole kidney. Most of these genes (displaying a tubule : whole kidney signal ratio of >5:1) were expressed in the proximal convoluted tubules. However, 9 genes (displaying a tubule : whole kidney signal ratio of <1:5) were expressed not in the proximal convoluted tubules but in the proximal straight tubule, another kidney segment, or in an identified region.

3.2. Microarray analysis of isolated proximal tubules from cisplatin-treated rats

To clarify the effects of various cisplatin doses on gene expression profiles in renal proximal tubules, we treated rats with cisplatin, 2 mg/kg or 10 mg/kg. The biochemical parameters of the animals 2 days after cisplatin administration are shown in Table 2. Plasma creatinine and blood urea nitrogen levels and creatinine clearance were comparable between sham-treated rats and the rats treated with 2 mg/kg cisplatin, whereas urinary albumin excretion was slightly increased in the latter group.

Conversely, rats treated with 10 mg/kg cisplatin showed severe nephrotoxicity. Plasma creatinine and blood urea nitrogen levels significantly increased, and body weight and creatinine clearance markedly decreased after treatment at this dose. Urinary albumin excretion was also significantly increased compared to sham-treated rats and rats treated with 2 mg/kg cisplatin.

Microarray analyses were performed on tubules isolated from sham- and cisplatin-treated rats. The gene numbers that changed significantly from the control were 311, 1961, and 1643 in the renal proximal tubules from rats treated with 2 and 10 mg/kg cisplatin and whole kidney from rats treated with 10 mg/kg cisplatin, respectively. Only 8 genes were commonly changed in the all 3 groups. Scatter plots of the gene expression signals from the isolated proximal tubules (rats treated with cisplatin, 2 mg/kg and 10 mg/kg) and whole kidney (rats treated with 10 mg/kg cisplatin) showed that the expression changes in rats treated with 2 mg/kg cisplatin were moderate compared with those of rats given 10 mg/kg cisplatin in comparisons with data from sham-operated rats. Conversely, 10 mg/kg cisplatin induced severe changes in gene expression in both isolated tubules and whole kidney.

3.3. Microarray analysis of the expression profile of signaling molecules

We then focused on signal-transducing molecules, selecting the genes in the proximal tubules or whole kidney that changed significantly and more than 2-fold with cisplatin treatment. Table 3 shows the 59 signaling molecules detected with this analysis. Among these, cytokines and chemokines were frequently increased in rats treated with 10 mg/kg cisplatin. The expression levels of 12 genes, including proinflammatory molecule IL-1beta and several chemokines (CCL2, CCL17, CCL19, CCL20, CXCL1,

CXCL2, CXCL10, and CXCL11) increased markedly ($P < 0.05$; >5-fold). Furthermore, the expression of 8 genes (*Bmp4*, *Egf*, *Lect2*, *Nrg1*, *Plcl1*, *Ppp1r1a*, *Tspan5*, *LOC307992*) significantly decreased to less than 20% of baseline ($P < 0.05$).

3.4. Changes in cytokine and chemokine expression in the kidneys of cisplatin-treated rats

Blood urea nitrogen and urinary albumin levels increased and creatinine clearance decreased in rats 4 days after treatment with 5 mg/kg cisplatin (Figure 1a). Furthermore, urinary *N*-acetyl-β-D-glucosaminidase activity increased the day after cisplatin administration. Histological analysis revealed few changes in the glomeruli, and moderate damage was observed in the proximal tubules 1 or 2 days after cisplatin administration (Figure 1b). Degeneration of tubular cells, demonstrated by brush border loss, tubular dilation, and cast formation, was most prominent 4 and 7 days post-treatment. These histological findings corresponded with changes in biochemical parameters, such as increased plasma creatinine and blood urea nitrogen levels.

Real-time PCR analyses using reverse-transcribed DNA samples prepared from whole kidneys were carried out to examine the changes in cytokine and chemokine expression associated with cisplatin-induced nephrotoxicity. The expression levels of IL-1beta, CCL2, CCL20, CXCL1, and CXCL10 were significantly increased with cisplatin treatment and peaked 4–7 days after the administration of 5 mg/kg of the drug (Figure 2).

3.5. Comparison of CCL2 and KIM-1 expression in the proximal tubules and whole kidney

The expression profiles of CCL2 and Kim-1 mRNA were compared in the isolated proximal tubules and whole kidney (Figures 3a and 3b). In whole-kidney samples, CCL2 mRNA levels decreased 1 and 2 days after treatment and then increased 4 and 7 days after treatment. Conversely, CCL2 expression gradually increased in the tubules immediately after cisplatin administration (Figure 3a) and Kim-1 expression increased greatly in a time-dependent manner in both the whole kidney and the tubules (Figure 3b). In addition, the expression profiles of CCL2 and KIM-1 proteins were compared (Figures 3c and 3d). In whole kidney lysate samples, CCL2 protein levels increased slightly 1 and 2 days after treatment and then peaked sharply 4 and 7 days after treatment (Figure 3c). KIM-1 protein expression was not detected at day 0, but it increased greatly by 7 days in a time-dependent manner (Figure 3d).

3.6. Time-dependent changes in CCL2 and KIM-1 protein expression and intra-renal distribution in rats with cisplatin nephropathy

Immunofluorescence analysis revealed CCL2 staining specifically in the cytoplasm of proximal tubules that was absent in the inner and outer medulla 1 and 2 days after cisplatin administration (Figure 4). CCL2 expression markedly increased in the proximal tubules, and strong CCL2 staining was observed in the interstitial region of the outer medulla on day 4. Furthermore, CCL2 expression decreased by day 7 in both the proximal tubules and the interstitial region of the outer medulla. No KIM-1 was detected in sham-treated rats (Figure 5). KIM-1 staining was observed in the apical membrane of proximal tubules in medulla at day 1 and 2, and KIM-1 expression decreased in a time-dependent manner and diffused to the superficial region. By day 7, the KIM-1 signal disappeared in the medulla and decreased in the cortex.

We also examined the localization of other cytokines and chemokines (Figure 6).

Immunofluorescence signals for IL-1beta (Figure 6a), CCL20 (Figure 6b), CXCL1

(Figure 6c), and CXCL10 (Figure 6d) were detected in the renal epithelial cells. The

reproducibility of immunofluorescence analyses was confirmed using several different

sections.

3.7. Increase in urinary CCL2 and KIM-1 levels in normal rats treated with cisplatin

Urinary CCL2 significantly increased the day after cisplatin administration to

approximately 3 times that observed in sham-treated rats (Figure 7a). CCL2 levels

further increased on day 2 and peaked on day 4. Measured urinary CCL2 excretion

corresponded well with the results of mRNA and immunofluorescence analyses.

However, plasma CCL2 levels remained constant in cisplatin-treated rats. Urinary

KIM-1 levels also significantly increased the day after cisplatin administration and

continued to rise with the deterioration of renal function (Figure 7b). Plasma creatinine

and blood urea nitrogen levels increased significantly on day 4 but did not change on

days 1 and 2 (Figure 7c).

3.8. Increase in urinary CCL2 and KIM-1 levels in chronic renal failure rats treated with cisplatin

Urinary CCL2 markedly increased the day after cisplatin administration to

approximately 4 times that observed in vehicle-treated chronic renal failure rats (Figure

8a). CCL2 levels increased further through day 7. Conversely, significant difference in

plasma CCL2 level was observed between vehicle-treated and cisplatin-administered

rats from days 2 to 7 (Figure 8b). Urinary KIM-1 levels in vehicle-treated chronic renal

failure rats gradually increased from days 4 to 7 with or without cisplatin administration (Figure 8c). Plasma creatinine and blood urea nitrogen levels did not significantly increase with or without cisplatin administration (Figure 8d). The renal expression level of OCT2 was similar between vehicle-treated and cisplatin-administered nephrectomized rats (data not shown).

4. Discussion

The renal proximal tubule is one of the kidney segments most susceptible to drug-induced injury because it concentrates numerous toxins [17]. In the present study, we successfully established an analytical system that focuses on gene expression in proximal tubules isolated by microdissection. As shown in Table 1, the signals of some Slc family transporters were higher in the proximal tubules than in whole kidney. The Na^+/D-glucose cotransporter (SGLT2/Slc5a2) is reported to be specifically localized to the S1 segment of renal proximal tubules; accordingly, in our microarray analysis, the SGLT2 mRNA signal in the proximal tubules was much higher than that in whole kidney. Conversely, the signal for the amino acid transporter Slc7a12, which is localized at the collecting ducts in the cortex, outer medulla, and inner medulla, was very low in the proximal tubules. Thus, microarray analysis using viable isolated proximal tubules can specifically reveal gene expression patterns in the renal proximal tubules without contamination from other nephron segments and infiltrating immune cells.

We have previously shown that renal cationic transporters determine the nephrotoxicity of cisplatin [5, 18, 19]. Cisplatin uptake, primarily by OCT2, and delay in tubular secretion by luminal H^+/organic cation antiporter/multidrug and toxin extrusion (MATE/SLC47A) causes drug accumulation and subsequent cytotoxicity in the proximal tubules in rats and humans. Concomitant administration of imatinib and cisplatin prevents cisplatin nephrotoxicity by inhibiting its OCT2-mediated basolateral uptake, thus preventing tubular injury [20]. In the present study, we used microarray analyses to clarify the changes in expression of tubular damage–specific genes in rats with cisplatin-induced nephrotoxicity. Intraperitoneal cisplatin administration resulted

in dose-dependent nephrotoxicity [5]. Renal proximal tubules are the primary site of drug-induced injury, followed by glomerular damage in cisplatin-induced nephropathy. Consistent with our results (see Table 3), those of a study by Ramesh and Reeves [21] showed activation of proinflammatory cytokines and chemokines in the kidneys of cisplatin-treated mice. Thus, enhanced cytokine and chemokine expression in proximal tubular epithelial cells is a major feature of cisplatin tubular toxicity.

To investigate time-dependent changes in the cytokines and chemokines, further experiments were conducted using rats treated with 5 mg/kg cisplatin, because of the poor survival of the rats treated with 10 mg/kg of cisplatin. Tubular injury became apparent earlier than a reduction in glomerular filtration rate in rats treated with 5 mg/kg cisplatin. Glomerular filtration rate reduction occurred on day 4, and renal function slightly improved on day 7. The mRNA expression profiles of IL-1beta, CCL2, CCL20, CXCL1, and CXCL10 were examined in the whole kidney to investigate the roles of cytokines and chemokines in the pathogenesis of cisplatin-induced nephrotoxicity (see Figure 2). The analysis revealed that the expression levels of these genes gradually increased 1–2 days after cisplatin treatment and peaked 4–7 days after treatment in parallel with the deterioration of renal function. A significant increase in CCL2 expression was detected in the proximal tubules the day after cisplatin administration, although CCL2 levels did not significantly increase in the whole kidney samples at this time (see Figure 3a). CCL2 mRNA levels markedly increased in both the proximal tubules and the whole kidney as did CCL2 protein in the whole kidney samples at the same time that blood urea nitrogen levels significantly increased and creatinine clearance decreased (see Figures 1a, 2b, 3a and 3c).

To obtain more detailed information, we determined the renal distribution of CCL2 protein through immunofluorescence analyses. CCL2 protein levels specifically and significantly increased in the tubular epithelium (see Figure 4). These results suggested that past studies using whole-kidney samples did not accurately detect segment-specific changes in CCL2 expression and missed early increases in CCL2 expression in the proximal tubules after cisplatin treatment. Furthermore, immunofluorescence analysis of other genes showed increases in IL-1beta, CCL20, CXCL1, and CXCL10 levels in tubular epithelial cells (see Figure 6) in agreement with the mRNA expression profiles of these proteins (see Figure 2), which were detected not only in the proximal tubules but also in the interstitial area of the medulla, suggesting that the proteins were secreted into the interstitium. These mediators may be essential factors for expanding immune cell–mediated renal inflammatory injury. There are numerous reports on the putative roles of CCL2 in renal diseases. CCL2 has been reported to be extensively involved in tubulointerstitial damage, including infiltration of monocytes and interstitial fibrosis in IgA nephropathy and diabetic nephropathy [22, 23]. Wada T at al. [24] showed that anti-CCL2 antibodies remarkably reduced glomerulosclerosis and improved renal dysfunction, as well as proteinuria in an animal model of crescentic glomerulonephritis, and similar renoprotective effects were observed in CCL2-depleted rats treated with the dominant negative gene of CCL2 [9]. Furthermore, the blockade of CCL2 signaling by CCR2 antagonist or CCR2 deletion showed a decrease in interstitial infiltrated macrophages in ischemia-reperfusion injury [25, 26]. Considering these reports, CCL2 might contribute to the development of renal injury as an exacerbation factor.

The expression of tumor necrosis factor (TNF)-alpha is reportedly important for the upstream regulation of proinflammatory cytokines [21, 27, 28]. Zhang et al. [29] have

shown that the production of TNF-alpha by renal parenchymal cells rather than by bone marrow–derived infiltrating immune cells is responsible for cisplatin-induced nephropathy. Although we found no increase in TNF-alpha mRNA in microarray analysis of isolated proximal tubules, the expression of several cytokines and chemokines markedly increased in renal epithelial cells. Taken together, these data suggest that renal epithelial cells may be an important source of several cytokines and chemokines that contribute to cisplatin-induced acute kidney injury.

KIM-1 (also known as hepatitis A virus receptor 1, Havcr1, or T-cell immunoglobulin and mucin, Tim-1), is a type I transmembrane protein undetectable in normal kidney tissue. Its expression increases in injured proximal tubular epithelial cells after ischemic or toxic injury [15]. The ectodomain of KIM-1 is stable in urine and can be detected both in the urine of patients with acute kidney injury [30] and in a variety of animal models of nephropathy induced by cisplatin [31, 32], S-(1,1,2,2,-tetrafluoroethyl)-L-cysteine, folic acid [31], and cyclosporine [33]. Urinary Kim-1 levels are exceptionally low under normal conditions but are highly induced immediately after tubular damage. Increased urinary KIM-1 occurs before increases in the levels of plasma creatinine and blood urea nitrogen in post-ischemic kidneys [32] and after a large number of toxins are released [15].

In the present study, renal mRNA expression and urinary excretion of KIM-1 were determined as references to evaluate the usefulness of examining CCL2 levels. Comparable to previous findings [31], Kim-1 mRNA and protein expression in the whole kidney samples and proximal tubules and KIM-1 urinary levels significantly increased the day after cisplatin administration (see Figures 3b, 3d, 5, and 7b). CCL2 expression predominantly increased in the proximal tubules (see Figures 3a and 4), and

similar to that of KIM-1, CCL2 excretion in the urine increased 1 day after cisplatin

treatment (see Figure 7a). Notably, KIM-1 and CCL2, which dominantly appeared in

the proximal tubules and urine before changes in blood urea nitrogen levels and

creatinine clearance, were observed after cisplatin treatment (see Figure 7c). Because

CCL2 was detected with immunofluorescence analysis only in the proximal epithelial

cells 1 and 2 days after cisplatin treatment, urinary CCL2 was derived from proximal

tubular epithelial cells and reflected tubular injury. In addition, urinary CCL2 rather

than KIM-1 increased for 7 days after low-dose administration of cisplatin (2 mg/kg) in

subtotal nephrectomized rats, whereas plasma levels of CCL2, creatinine, and blood

urea nitrogen were constant (see Figure 8). In progressive chronic renal failure rats,

urinary levels of KIM-1 were rapidly increased by treatment of cisplatin, but its level

also gradually increased without cisplatin treatment (see Figure 8c). Therefore, the

additional increase of KIM-1 by cisplatin treatment was considered to be small,

suggesting that urinary KIM-1 levels reflected the sum of cisplatin-induced

nephrotoxicity and accumulating tubular damage by subtotal nephrectomy. On the other

hand, urinary levels of CCL2 were supposed to be associated with the dosage of

cisplatin (5 mg/kg in Figure 7a; 2 mg/kg in Figure 8a) regardless of subtotal

nephrectomy. These results indicated that compared with urinary KIM-1, increased

urinary CCL2 was relatively selective for cisplatin-induced nephrotoxicity, and

therefore, expression of renal CCL2 might be induced in association with renal

accumulation of cisplatin. Some reports have associated urinary CCL2 with some renal

diseases. In patients with IgA nephropathy or lupus nephritis, urinary CCL2 is increased

and related to disease stage [34-39]. In addition to its presence in these autoimmune

diseases, CCL2 has been detected in the urine of patients with diabetic nephropathy [40]

and polycystic kidney disease [41]. Recently, urinary CCL2 has been identified as a marker of renal function decline in diabetic and nondiabetic proteinuric renal disease independent from and additive to proteinuria [42]. These reports suggest that CCL2 might be associated with the pathogenesis of several kidney diseases and be a relatively stable biomarker in patient urine samples. Taken together, the combination of urinary CCL2 and Kim-1 may be a more sensitive and specific biomarker for cisplatin-induced nephrotoxicity, especially in patients with renal impairment.

In conclusion, microarray analysis with isolated proximal tubules was useful to detect specific responses in intact proximal tubules after renal injury. Furthermore, increases in inflammatory cytokines and chemokines in the proximal tubules preceded kidney functional changes observed with the progression of cisplatin-induced nephropathy. Although further validation with clinical samples is needed, urinary CCL2 and Kim-1 might be non-invasive biomarkers for detecting cisplatin-induced tubular toxicity in humans.

Acknowledgement

Disclosure

JVB is a co-inventor on KIM-1 patents that are assigned to Partners Healthcare and licensed by Partners to Johnson and Johnson, Sekisui, BiogenIdec and a number of research reagent companies. JVB is a consultant for Sekisui. The other authors declare no conflict of interest with third parties.

Authorship

(1) Study conception and design: K.N., S.M.

(2) Acquisition, analysis and/or interpretation of data: K.N., H.S., A.O., A.Y., S.N. S.M.

(3) Drafting/revision of the work for intellectual content and context: K.N., T.I., J.V.B., K.M., K.I., S.M.

(4) Final approval and overall responsibility for the published work: S.M.

References

[1]   Perazella MA. Renal vulnerability to drug toxicity. Clin J Am Soc Nephrol 2009;4:1275-83.

[2]   Mehta RL, Pascual MT, Soroko S, Savage BR, Himmelfarb J, Ikizler TA, et al. Spectrum of acute renal failure in the intensive care unit: the PICARD experience. Kidney Int 2004;66:1613-21.

[3]   Inui K, Masuda S, Saito H. Cellular and molecular aspects of drug transport in the kidney. Kidney Int 2000;58:944-58.

[4]   Williams CJ, Whitehouse JM. Cis-platinum: a new anticancer agent. Br Med J 1979;1:1689-91.

[5]   Yonezawa A, Masuda S, Nishihara K, Yano I, Katsura T, Inui K. Association between tubular toxicity of cisplatin and expression of organic cation transporter rOCT2 (Slc22a2) in the rat. Biochem Pharmacol 2005;70:1823-31.

[6]   Yao X, Panichpisal K, Kurtzman N, Nugent K. Cisplatin nephrotoxicity: a review. Am J Med Sci 2007;334:115-24.

[7]   Cornelison TL, Reed E. Nephrotoxicity and hydration management for cisplatin, carboplatin, and ormaplatin. Gynecol Oncol 1993;50:147-58.

[8]   Nishihara K, Masuda S, Nakagawa S, Yonezawa A, Ichimura T, Bonventre JV, et al. Impact of Cyclin B2 and Cell division cycle 2 on tubular hyperplasia in progressive chronic renal failure rats. Am J Physiol Renal Physiol 2010;298:F923-F34.

[9]   Wada T, Furuichi K, Sakai N, Iwata Y, Kitagawa K, Ishida Y, et al. Gene therapy via blockade of monocyte chemoattractant protein-1 for renal fibrosis. J Am Soc Nephrol 2004;15:940-8.

[10] Masuda S, Saito H, Nonoguchi H, Tomita K, Inui K. mRNA distribution and membrane localization of the OAT-K1 organic anion transporter in rat renal tubules. FEBS Lett 1997;407:127-31.

[11] Nakagawa S, Masuda S, Nishihara K, Inui K. mTOR inhibitor everolimus ameliorates progressive tubular dysfunction in chronic renal failure rats. Biochem Pharmacol 2010;79:67-76.

[12] Zager RA, Johnson AC, Hanson SY, Lund S. Acute nephrotoxic and obstructive injury primes the kidney to endotoxin-driven cytokine/chemokine production. Kidney Int 2006;69:1181-8.

[13] Nakagawa S, Nishihara K, Inui K, Masuda S. Involvement of autophagy in the pharmacological effects of the mTOR inhibitor everolimus in acute kidney injury. Eur J Pharmacol 2012;696:143-54.

[14] Prozialeck WC, Vaidya VS, Liu J, Waalkes MP, Edwards JR, Lamar PC, et al. Kidney injury molecule-1 is an early biomarker of cadmium nephrotoxicity. Kidney Int 2007;72:985-93.

[15] Vaidya VS, Ozer JS, Dieterle F, Collings FB, Ramirez V, Troth S, et al. Kidney injury molecule-1 outperforms traditional biomarkers of kidney injury in preclinical biomarker qualification studies. Nat Biotechnol 2010;28:478-85.

[16] Ji L, Masuda S, Saito H, Inui K. Down-regulation of rat organic cation transporter rOCT2 by 5/6 nephrectomy. Kidney Int 2002;62:514-24.

[17] Bonventre JV, Vaidya VS, Schmouder R, Feig P, Dieterle F. Next-generation biomarkers for detecting kidney toxicity. Nat Biotechnol 2010;28:436-40.

[18] Yonezawa A, Masuda S, Yokoo S, Katsura T, Inui K. Cisplatin and oxaliplatin, but not carboplatin and nedaplatin, are substrates for human organic cation transporters

(SLC22A1-3 and multidrug and toxin extrusion family). J Pharmacol Exp Ther 2006;319:879-86.

[19]   Yokoo S, Yonezawa A, Masuda S, Fukatsu A, Katsura T, Inui K. Differential contribution of organic cation transporters, OCT2 and MATE1, in platinum agent-induced nephrotoxicity. Biochem Pharmacol 2007;74:477-87.

[20]   Tanihara Y, Masuda S, Katsura T, Inui K. Protective effect of concomitant administration of imatinib on cisplatin-induced nephrotoxicity focusing on renal organic cation transporter OCT2. Biochem Pharmacol 2009;78:1263-71.

[21]   Ramesh G, Reeves WB. TNF-alpha mediates chemokine and cytokine expression and renal injury in cisplatin nephrotoxicity. J Clin Invest 2002;110:835-42.

[22]   Hagiwara S, Makita Y, Gu L, Tanimoto M, Zhang M, Nakamura S, et al. Eicosapentaenoic acid ameliorates diabetic nephropathy of type 2 diabetic KKAy/Ta mice: involvement of MCP-1 suppression and decreased ERK1/2 and p38 phosphorylation. Nephrol Dial Transplant 2006;21:605-15.

[23]   Ou ZL, Hotta O, Natori Y, Sugai H, Taguma Y. Enhanced expression of C chemokine lymphotactin in IgA nephropathy. Nephron 2002;91:262-9.

[24]   Wada T, Yokoyama H, Furuichi K, Kobayashi KI, Harada K, Naruto M, et al. Intervention of crescentic glomerulonephritis by antibodies to monocyte chemotactic and activating factor (MCAF/MCP-1). FASEB J 1996;10:1418-25.

[25]   Li L, Huang L, Sung SS, Vergis AL, Rosin DL, Rose CE, Jr., et al. The chemokine receptors CCR2 and CX3CR1 mediate monocyte/macrophage trafficking in kidney ischemia-reperfusion injury. Kidney Int 2008;74:1526-37.

[26]   Furuichi K, Wada T, Iwata Y, Kitagawa K, Kobayashi K, Hashimoto H, et al. CCR2

signaling contributes to ischemia-reperfusion injury in kidney. J Am Soc Nephrol

2003;14:2503-15.

[27]   Kelly KJ, Meehan SM, Colvin RB, Williams WW, Bonventre JV. Protection from

toxicant-mediated renal injury in the rat with anti-CD54 antibody. Kidney Int

1999;56:922-31.

[28]   Ramesh G, Reeves WB. Salicylate reduces cisplatin nephrotoxicity by inhibition of

tumor necrosis factor-alpha. Kidney Int 2004;65:490-9.

[29]   Zhang B, Ramesh G, Norbury CC, Reeves WB. Cisplatin-induced nephrotoxicity is

mediated by tumor necrosis factor-α produced by renal parenchymal cells. Kidney Int

2007;72:37-44.

[30]   Han WK, Bailly V, Abichandani R, Thadhani R, Bonventre JV. Kidney Injury

Molecule-1 (KIM-1): a novel biomarker for human renal proximal tubule injury.

Kidney Int 2002;62:237-44.

[31]   Ichimura T, Hung CC, Yang SA, Stevens JL, Bonventre JV. Kidney injury molecule-1:

a tissue and urinary biomarker for nephrotoxicant-induced renal injury. Am J Physiol

Renal Physiol 2004;286:F552-63.

[32]   Vaidya VS, Ramirez V, Ichimura T, Bobadilla NA, Bonventre JV. Urinary kidney

injury molecule-1: a sensitive quantitative biomarker for early detection of kidney

tubular injury. Am J Physiol Renal Physiol 2006;290:F517-29.

[33]   Perez-Rojas J, Blanco JA, Cruz C, Trujillo J, Vaidya VS, Uribe N, et al.

Mineralocorticoid receptor blockade confers renoprotection in preexisting chronic

cyclosporine nephrotoxicity. Am J Physiol Renal Physiol 2007;292:F131-9.

[34]   Noris M, Bernasconi S, Casiraghi F, Sozzani S, Gotti E, Remuzzi G, et al. Monocyte

chemoattractant protein-1 is excreted in excessive amounts in the urine of patients with

lupus nephritis. Lab Invest 1995;73:804-9.

[35]   Wada T, Yokoyama H, Su SB, Mukaida N, Iwano M, Dohi K, et al. Monitoring urinary

levels of monocyte chemotactic and activating factor reflects disease activity of lupus

nephritis. Kidney Int 1996;49:761-7.

[36]   Saitoh A, Suzuki Y, Takeda M, Kubota K, Itoh K, Tomino Y. Urinary levels of

monocyte chemoattractant protein (MCP)-1 and disease activity in patients with IgA

nephropathy. J Clin Lab Anal 1998;12:1-5.

[37]   Rovin BH, Song H, Birmingham DJ, Hebert LA, Yu CY, Nagaraja HN. Urine

chemokines as biomarkers of human systemic lupus erythematosus activity. J Am Soc

Nephrol 2005;16:467-73.

[38]   Torres DD, Rossini M, Manno C, Mattace-Raso F, D'Altri C, Ranieri E, et al. The ratio

of epidermal growth factor to monocyte chemotactic peptide-1 in the urine predicts

renal prognosis in IgA nephropathy. Kidney Int 2008;73:327-33.

[39]   Kiani AN, Johnson K, Chen C, Diehl E, Hu H, Vasudevan G, et al. Urine

osteoprotegerin and monocyte chemoattractant protein-1 in lupus nephritis. J Rheumatol

2009;36:2224-30.

[40]   Tesch GH. MCP-1/CCL2: a new diagnostic marker and therapeutic target for

progressive renal injury in diabetic nephropathy. Am J Physiol Renal Physiol

2008;294:F697-701.

[41]   Zheng D, Wolfe M, Cowley BD, Jr., Wallace DP, Yamaguchi T, Grantham JJ. Urinary

excretion of monocyte chemoattractant protein-1 in autosomal dominant polycystic

kidney disease. J Am Soc Nephrol 2003;14:2588-95.

[42]   Camilla R, Brachemi S, Pichette V, Cartier P, Laforest-Renald A, Macrae T, et al.
Urinary monocyte chemotactic protein 1: marker of renal function decline in diabetic
and nondiabetic proteinuric renal disease. J Nephrol 2010.

[43]   Cramer SC, Pardridge WM, Hirayama BA, Wright EM. Colocalization of GLUT2
glucose transporter, sodium/glucose cotransporter, and gamma-glutamyl transpeptidase
in rat kidney with double-peroxidase immunocytochemistry. Diabetes 1992;41:766-70.

[44]   Ramadan T, Camargo SM, Summa V, Hunziker P, Chesnov S, Pos KM, et al.
Basolateral aromatic amino acid transporter TAT1 (Slc16a10) functions as an efflux
pathway. J Cell Physiol 2006;206:771-9.

[45]   Roussa E, Nastainczyk W, Thevenod F. Differential expression of electrogenic NBC1
(SLC4A4) variants in rat kidney and pancreas. Biochem Biophys Res Commun
2004;314:382-9.

[46]   You G, Lee WS, Barros EJ, Kanai Y, Huo TL, Khawaja S, et al. Molecular
characteristics of Na^+-coupled glucose transporters in adult and embryonic rat kidney. J
Biol Chem 1995;270:29365-71.

[47]   Bauch C, Forster N, Loffing-Cueni D, Summa V, Verrey F. Functional cooperation of
epithelial heteromeric amino acid transporters expressed in madin-darby canine kidney
cells. J Biol Chem 2003;278:1316-22.

[48]   Chairoungdua A, Segawa H, Kim JY, Miyamoto K, Haga H, Fukui Y, et al.
Identification of an amino acid transporter associated with the cystinuria-related type II
membrane glycoprotein. J Biol Chem 1999;274:28845-8.

[49]   Biemesderfer D, Rutherford PA, Nagy T, Pizzonia JH, Abu-Alfa AK, Aronson PS.
Monoclonal antibodies for high-resolution localization of NHE3 in adult and neonatal
rat kidney. Am J Physiol 1997;273:F289-99.

[50]   Custer M, Murer H, Biber J. Nephron localization of Na^+/SO_4^{2-}-cotransport-related

mRNA and protein. Pflugers Arch 1994;429:165-8.

[51]   Shen H, Smith DE, Yang T, Huang YG, Schnermann JB, Brosius FC, 3rd. Localization

of PEPT1 and PEPT2 proton-coupled oligopeptide transporter mRNA and protein in rat

kidney. Am J Physiol 1999;276:F658-65.

[52]   Yanase H, Takebe K, Nio-Kobayashi J, Takahashi-Iwanaga H, Iwanaga T. Cellular

expression of a sodium-dependent monocarboxylate transporter (Slc5a8) and the MCT

family in the mouse kidney. Histochem Cell Biol 2008;130:957-66.

[53]   Urakami Y, Okuda M, Masuda S, Akazawa M, Saito H, Inui K. Distinct characteristics

of organic cation transporters, OCT1 and OCT2, in the basolateral membrane of renal

tubules. Pharm Res 2001;18:1528-34.

[54]   Wu X, Huang W, Prasad PD, Seth P, Rajan DP, Leibach FH, et al. Functional

characteristics and tissue distribution pattern of organic cation transporter 2 (OCTN2),

an organic cation/carnitine transporter. J Pharmacol Exp Ther 1999;290:1482-92.

[55]   Hasegawa M, Kusuhara H, Sugiyama D, Ito K, Ueda S, Endou H, et al. Functional

involvement of rat organic anion transporter 3 (rOat3; Slc22a8) in the renal uptake of

organic anions. J Pharmacol Exp Ther 2002;300:746-53.

[56]   Karniski LP, Lotscher M, Fucentese M, Hilfiker H, Biber J, Murer H.

Immunolocalization of sat-1 sulfate/oxalate/bicarbonate anion exchanger in the rat

kidney. Am J Physiol 1998;275:F79-87.

[57]   Kim YH, Kwon TH, Frische S, Kim J, Tisher CC, Madsen KM, et al.

Immunocytochemical localization of pendrin in intercalated cell subtypes in rat and

mouse kidney. Am J Physiol Renal Physiol 2002;283:F744-54.

[58]   Rodriguez-Mulero S, Errasti-Murugarren E, Ballarin J, Felipe A, Doucet A, Casado FJ,

et al. Expression of concentrative nucleoside transporters SLC28 (CNT1, CNT2, and

CNT3) along the rat nephron: effect of diabetes. Kidney Int 2005;68:665-72.

[59]   Breusegem SY, Takahashi H, Giral-Arnal H, Wang X, Jiang T, Verlander JW, et al.

Differential regulation of the renal sodium-phosphate cotransporters NaPi-IIa, NaPi-IIc,

and PiT-2 in dietary potassium deficiency. Am J Physiol Renal Physiol

2009;297:F350-61.

[60]   Praetorius J, Kim YH, Bouzinova EV, Frische S, Rojek A, Aalkjaer C, et al. NBCn1 is

a basolateral Na^+-HCO_3^- cotransporter in rat kidney inner medullary collecting ducts.

Am J Physiol Renal Physiol 2004;286:F903-12.

[61]   Chairoungdua A, Kanai Y, Matsuo H, Inatomi J, Kim DK, Endou H. Identification and

characterization of a novel member of the heterodimeric amino acid transporter family

presumed to be associated with an unknown heavy chain. J Biol Chem

2001;276:49390-9.

[62]   Matsuo H, Kanai Y, Kim JY, Chairoungdua A, Kim DK, Inatomi J, et al. Identification

of a novel Na^+-independent acidic amino acid transporter with structural similarity to

the member of a heterodimeric amino acid transporter family associated with unknown

heavy chains. J Biol Chem 2002;277:21017-26.

[63]   Anzai N, Jutabha P, Enomoto A, Yokoyama H, Nonoguchi H, Hirata T, et al.

Functional characterization of rat organic anion transporter 5 (Slc22a19) at the apical

membrane of renal proximal tubules. J Pharmacol Exp Ther 2005;315:534-44.

[64]   Ljubojevic M, Balen D, Breljak D, Kusan M, Anzai N, Bahn A, et al. Renal expression

of organic anion transporter OAT2 in rats and mice is regulated by sex hormones. Am J

Physiol Renal Physiol 2007;292:F361-72.

Table 1. Comparison of the solute carrier family expression levels in isolated proximal tubules and whole kidney.

Probe ID	Gene Symbol	Ratio	P value	RefSeqs	Renal distribution	Reference
Proximal tubule > Whole kidney						
20931266	Slc2a2	9.8	0.000	NM_012879.1	PCT	[43]
21588487	Slc3a2	8.5	0.002	NM_019283.1	PCT (mouse)	[44]
21943154	Slc4a4	50.5	0.001	NM_053424.1	PCT	[45]
22386465	Slc5a2	491.3	0.000	NM_022590.2	PCT	[46]
21957982	Slc6a8	5.9	0.029	XM_579415	N.A.	-
20879733	Slc7a7	150.5	0.000	NM_031341.1	PCT (mouse)	[47]
21509630	Slc7a9	15.2	0.003	NM_053929.1	PCT	[48]
21041351	Slc9a3	6.2	0.000	XM_579341	PCT	[49]
20742389	Slc12a8	11.0	0.000	NM_153625.1	N.A.	-
21280496	Slc13a1	11.9	0.000	NM_031651.1	PCT	[50]
20808386	Slc15a1	44.2	0.002	NM_057121.1	PCT	[51]
21184793	Slc16a1	79.5	0.002	NM_012716.1	PCT (mouse)	[52]
20744521	Slc16a6	18.1	0.043	NM_198760.1	N.A.	-
21014572	Slc16a14	11.5	0.001	NM_001108229.1	N.A.	-
21479059	Slc22a1	6.4	0.000	NM_012697.1	PCT	[53]
21858745	Slc22a5	6.9	0.009	NM_019269.1	PCT	[54]
20967193	Slc22a8	8.4	0.018	NM_031332.1	PCT	[55]
22122470	Slc26a1	6.0	0.027	NM_022287.1	PCT	[56]
21788690	Slc26a4	7.7	0.060	NM_019214.1	CCD	[57]
20797965	Slc28a2	5.2	0.002	NM_031664.1	PCT, PST, OMCD	[58]

22191184	Slc30a2	8.6	0.008	NM_012890.1	N.A.	-
22298458	Slc32a1	7.1	0.241	NM_031782.1	N.A.	-
21770029	Slc34a3	8.0	0.000	NM_139338.1	PCT	[59]
Proximal tubule < Whole kidney						
21160091	Slc4a11	0.087	0.113	XM_230605	IMCD	[60]
22351360	Slc7a12	0.038	0.011	NM_001011948.1	CCD, OMCD, IMCD (mouse)	[61]
21486326	Slc7a13	0.120	0.010	XM_575781	PST, DCT (mouse)	[62]
21875597	Slc21a13	0.168	0.037	NM_130736.1	N.A.	-
21666827	Slc22a19	0.147	0.012	XM_342011	PST	[63]
21889439	Slc22a7	0.151	0.009	NM_053537.1	PST	[64]
21624701	Slc23a3	0.142	0.041	XM_346061	N.A.	-
21018836	Slc34a2	0.125	0.037	XM_579555	N.A.	-
21451109	Slc41a2	0.164	0.122	NM_001108742.1	N.A.	-

The expression levels of solute carrier (Slc) family genes were examined and compared by microarray analysis. The ratios of proximal tubule:whole kidney mRNA expression levels are also presented. PCT, proximal convoluted tubule; CCD, cortical collecting duct; PST, proximal straight tubule; OMCD, outer medullary collecting duct; IMCD, inner medullary collecting duct; TAL, thick ascending limb; DCT, distal connecting tubule; N.A., not available.

Table 2. Biochemical parameters of cisplatin-treated rats.[a]

Parameter	Units	Sham[b]	Cisplatin	
			2 mg/kg	10 mg/kg
Body weight	G	282 ± 4	279 ± 3	248 ± 4**
Plasma creatinine	mg/dL	0.52 ± 0.07	0.54 ± 0.04	0.90 ± 0.05**
Creatinine clearance	ml/min	1.34 ± 0.15	1.50 ± 0.05	0.70 ± 0.08**
Blood urea nitrogen	mg/dL	14.4 ± 0.9	17.5 ± 0.1	46.6 ± 2.0**
Albumin excretion	mg/day	0.39 ± 0.11	0.81 ± 0.62*	9.67 ± 2.10*

Blood and urine samples were obtained from cisplatin-treated rats 2 days after cisplatin administration.
[a]Each value represents mean ± standard error; multiple comparisons were performed with Dunnett's 2-tailed test after 1-way analysis of variance. [b]Sham, vehicle-treated rats. *$P < 0.05$, **$P < 0.01$, significantly different from sham-treated rats.

Table 3. Changes in signaling molecule expression levels in cisplatin-treated rats.

| Probe ID | Gene symbol | Gene name | Proximal tubule | | | | Whole kidney | | RefSeqs |
| | | | 2 mg/kg | | 10 mg/kg | | 10 mg/kg | | |
			Ratio	P value	Ratio	P value	Ratio	P value	
21531200	*Abtb2*	Ankyrin repeat and BTB (POZ) domain containing 2	1.03	0.8936	**0.34**	**0.0062**	**0.34**	**0.0443**	NM_134403.1
21031514	*Adm*	Adrenomedullin	1.04	0.9232	**4.11**	**0.0326**	**6.93**	**0.0193**	NM_012715.1
21515889	*Angptl4*	Angiopoietin-like protein 4	0.54	0.6372	**6.54**	**0.0185**	**11.69**	**0.0146**	NM_199115.2
21706219	*Bcl2*	B-cell leukemia/lymphoma 2	1.28	0.1133	**0.29**	**0.0011**	1.62	0.1996	NM_016993.1
21567665	*Bcl2l1*	Bcl2-like 1	1.04	0.8814	**0.34**	**0.0062**	0.62	0.1152	NM_001033670.1
22406016	*Bcl2l2*	Bcl2-like 2	1.81	0.1308	**2.65**	**0.0162**	**4.42**	**0.0443**	NM_021850.2
21591819	*Blnk*	B-cell linker	0.81	0.4571	**2.94**	**0.0101**	**4.38**	**0.0106**	NM_001025767.1
21743176	*Bmp2*	Bone morphogenetic protein 2	**2.66**	**0.0407**	**3.35**	**0.0149**	2.60	0.1146	NM_017178.1
20823942	*Bmp4*	Bone morphogenetic protein 4	2.10	0.0859	**0.40**	**0.0838**	**0.08**	**0.0182**	NM_012827.1
20907835	*Ccl2*	Chemokine (C-C motif) ligand 2	2.60	0.2375	**9.33**	**0.0047**	**3.36**	**0.0096**	NM_031530.1
22219977	*Ccl17*	Small inducible cytokine subfamily A (Cys-Cys), member 17	1.03	0.9591	1.22	0.5490	**3.21**	**0.0041**	NM_057151.1
21438363	*Ccl19*	Chemokine (C-C motif) ligand 19	1.28	0.4879	**7.07**	**0.0159**	**10.02**	**0.0211**	XM_342824
21035433	*Ccl20*	Chemokine (C-C motif) ligand 20	0.83	0.7799	**25.34**	**0.0112**	**20.12**	**0.0034**	NM_019233.1
22317053	*Cxcl1*	Chemokine (C-X-C motif) ligand 1	2.32	0.2819	**25.16**	**0.0211**	5.19	0.0776	NM_030845.1
20807096	*Cxcl2*	Chemokine (C-X-C motif) ligand 2	1.93	0.3376	**5.50**	**0.0163**	**4.22**	**0.0093**	NM_053647.1
21382174	*Cxcl10*	Chemokine (C-X-C motif) ligand 10	0.45	0.5638	**7.60**	**0.0494**	**12.08**	**0.0131**	NM_139089.1
21707155	*Cxcl11*	Chemokine (C-X-C motif) ligand 11	1.06	0.8853	6.48	0.0762	**4.13**	**0.0438**	NM_182952.2
20983420	*Dtr*	Diphtheria toxin receptor	1.46	0.3258	**15.83**	**0.0155**	**10.18**	**0.0018**	NM_012945.1
21546114	*Egf*	Epidermal growth factor	0.69	0.3589	**0.19**	**0.0443**	**0.10**	**0.0157**	NM_012842.1
21186251	*Elmo3*	Engulfment and cell motility 3, ced-12 homolog (*Caenorhabditis elegans*)	1.17	0.7562	1.02	0.9676	**0.22**	**0.0042**	NM_001030028.1
21470303	*Esm1*	Endothelial cell-specific molecule 1	0.87	0.5572	0.88	0.6551	**0.40**	**0.0263**	NM_022604.2

21964976	Fgb	Fibrinogen, B beta polypeptide	1.05	0.8336	**18.78**	**0.0284**	**4.32**	**0.0373**	NM_020071.1
21518483	Fgf9	Fibroblast growth factor 9	1.54	0.0009	**0.37**	**0.0040**	0.51	0.0651	NM_012952.1
21812027	Fgf13	Fibroblast growth factor 13	1.67	0.1527	**0.46**	**0.0254**	0.43	0.2588	NM_053428.1
21487754	Fgf22	Fibroblast growth factor 22	0.60	0.2978	**2.96**	**0.0209**	0.73	0.0758	NM_130751.1
21189934	Glg1	Golgi apparatus protein 1	1.04	0.8620	**0.32**	**0.0140**	0.51	0.0738	NM_017211.1
21900160	Grb2	Growth factor receptor bound protein 2	1.16	0.4897	**0.47**	**0.0207**	**0.37**	**0.0245**	NM_030846.2
22276618	Grip1	Glutamate receptor interacting protein 1	1.63	0.1956	1.92	0.2164	**4.66**	**0.0000**	NM_032069.1
21999055	Igf1	Insulin-like growth factor 1	0.53	0.3679	0.37	0.2397	**0.29**	**0.0368**	NM_178866.2
21698275	Il1b	Interleukin 1 beta	2.67	0.1913	**5.75**	**0.0217**	1.90	0.1502	NM_031512.1
21788366	Lect2	Leukocyte cell-derived chemotaxin 2	0.75	0.4936	**0.16**	**0.0065**	**2.32**	**0.0009**	XM_341486
21243387	Lgals1	Lectin, galactose binding, soluble 1	0.80	0.6196	1.85	0.1189	**2.40**	**0.0046**	NM_019904.1
21739265	Lgals3	Lectin, galactose binding, soluble 3	0.91	0.5875	1.97	0.0679	**3.05**	**0.0321**	NM_031832.1
20916699	Mia2	Melanoma inhibitory activity 2	1.29	0.4184	**0.42**	**0.0261**	1.22	0.6230	XM_343068
21951725	Nrg1	Neuregulin 1	1.63	0.2596	2.63	0.1390	**0.13**	**0.0006**	NM_031588.1
21435765	Numb	Numb gene homolog (*Drosophila*)	1.01	0.9668	**0.37**	**0.0043**	0.47	0.1130	NM_133287.1
20878482	Pdgfa	Platelet derived growth factor, alpha	0.75	0.1553	**2.84**	**0.0082**	1.59	0.0998	NM_012801.1
20800589	Pdgfc	Platelet-derived growth factor, C polypeptide	**2.53**	**0.0370**	**0.25**	**0.0069**	0.90	0.7311	NM_031317.1
21861133	Pf4	Platelet factor 4	0.70	0.3276	1.05	0.8315	**2.59**	**0.0041**	NM_001007729.1
22197072	Plcl1	Phospholipase C-like 1	0.88	0.7009	**0.12**	**0.0184**	0.58	0.1968	NM_053456.1
21720242	Ppp1r1a	Protein phosphatase 1, regulatory (inhibitor) subunit 1A	0.64	0.4995	0.13	0.1390	**0.13**	**0.0304**	NM_022676.3
21554485	Psmc	Pre-sialomucin complex	0.95	0.8944	1.37	0.1147	**0.37**	**0.0084**	XM_221384
21725361	Pzp	Pregnancy-zone protein	1.11	0.6942	**0.08**	**0.0125**	**0.27**	**0.0353**	NM_145779.1
21579013	S100a11	S100 calcium binding protein A11 (calizzarin; predicted)	0.92	0.6850	5.65	0.1203	**4.49**	**0.0005**	NM_001004095.1
21687629	Skb1	SKB1 homolog (*Schizosaccharomyces pombe*) (predicted)	0.94	0.6836	**2.10**	**0.0104**	1.37	0.4582	XM_344405
21897732	Stambp	Associated molecule with the SH3 domain	1.17	0.5004	0.59	0.0806	**0.49**	**0.0111**	NM_138531.2

		of signal-transducing adaptor molecule							
22350958	*Tgfb2*	Transforming growth factor, beta 2	0.88	0.2299	**0.39**	**0.0257**	1.35	0.5971	NM_031131.1
21911962	*Tgfbi*	Transforming growth factor, beta induced	0.59	0.5430	0.32	0.2984	**0.21**	**0.0338**	XM_573983
21715280	*Traf3*	TNF receptor-associated factor 3 (predicted)	0.99	0.9624	0.52	0.0157	**0.49**	**0.0230**	NM_001108724.1
22166383	*Trip10*	Thyroid hormone receptor interactor 10	2.11	0.1552	**3.82**	**0.0243**	1.92	0.2074	XM_579584
20717612	*Tspan5*	Tetraspanin 5	1.34	0.5546	**0.16**	**0.0331**	**0.23**	**0.0199**	NM_001004090.2
21728398	*Vgf*	VGF nerve growth factor inducible	0.71	0.4607	**2.77**	**0.0184**	1.66	0.4020	NM_030997.1
21940318	*Wisp1*	WNT1 inducible signaling pathway protein 1	0.47	0.1464	0.72	0.5068	**3.28**	**0.0104**	NM_031716.1
21513214	*Wnt2*	Wingless-related MMTV integration site 2	0.85	0.7417	**2.86**	**0.0330**	2.76	0.0751	XM_575397
22317272	*LOC307992*		0.76	0.1111	**0.07**	**0.0006**	0.43	0.0565	
22403887	*LOC500065*		1.29	0.0255	**0.32**	**0.0007**	0.61	0.1281	XM_575419
21901355			1.36	0.2174	**3.86**	**0.0386**	**3.89**	**0.0003**	
20901294			1.92	0.0193	**0.39**	**0.0095**	**3.60**	**0.0024**	
21070158			0.95	0.6891	1.06	0.6784	**2.10**	**0.0458**	

Proximal tubules and whole kidney samples were obtained from cisplatin-treated rats 2 days after cisplatin administration and microarray analyses were performed. Focusing on the signaling molecules, we determined the mRNA expression level ratio between cisplatin-treated and sham-treated rats and calculated P values with 1-way analysis of variance. $P < 0.05$ was considered statistically significant. Bold type indicates the genes that changed more than 2-fold, with a P value of <0.05.

Figure Legends

Figure <u>1</u>. Time-dependent changes in renal function and histology of rats treated with 5 mg/kg cisplatin. The changes in creatinine clearance (Ccr), blood urea nitrogen (BUN), urinary excretion of albumin, and urinary *N*-acetyl-β-D-glucosaminidase (NAG) activity 1, 2, 4, and 7 days after cisplatin administration are shown (**a**). Histological analyses of the kidneys are also shown (**b**). *, glomeruli. Data are expressed as means ± standard error (S.E.) of 6 rats. Multiple comparisons were performed with Dunnett's 2-tailed test after 1-way analysis of variance (ANOVA). * $P < 0.05$, **$P < 0.01$, significantly different from the value on day 0.

Figure <u>2</u>. Cytokine and chemokine expression profiles of rats treated with 5 mg/kg cisplatin. Interleukin (IL)-1beta (**a**), chemokine (C-C motif) ligand (CCL) 2 (**b**), CCL20 (**c**), chemokine (C-X-C motif) ligand (CXCL) 1 (**d**), and CXCL10 (**e**) mRNA levels were examined. Whole-kidney total RNA was extracted from rats 1, 2, 4, and 7 days after cisplatin treatment and reverse-transcribed to complementary DNA (cDNA). Real-time PCR analysis was performed using these cDNAs. Glyceraldehyde-3-phosphate dehydrogenase (GAPDH) mRNA was used as an internal control. Data are expressed as means ± S.E. of 6 rats. Multiple comparisons were performed with Dunnett's 2-tailed test after 1-way ANOVA. *$P < 0.05$, **$P < 0.01$, significantly different from the value on day 0.

Figure <u>3</u>. Comparison of CCL2 and kidney injury molecule-1 (Kim-1) <u>expression in the</u> kidney. (**a**) and (**b**), Total RNA was extracted from isolated proximal tubules

(***open circles***) and whole kidneys (***closed circles***) of rats treated with 5 mg/kg cisplatin. This RNA was reverse-transcribed to yield cDNA. Real-time polymerase chain reaction analysis of CCL2 (**a**) and Kim-1 (**b**) was performed using these cDNAs. GAPDH mRNA was used as an internal control. Ratio to day 0 was calculated, and data are expressed as means ± S.E. of 3–5 rats. Multiple comparisons were performed with Dunnett's 2-tailed test after 1-way ANOVA. $*P < 0.05$, $**P < 0.01$, significantly different from the value at day 0. (**c**) and (**d**), Lysate samples were prepared from whole kidneys of rats treated with 5 mg/kg cisplatin. CCL2 concentrations were measured using enzyme-linked immunosorbent assay (ELISA) kits (**c**), and Kim-1 levels were determined with microsphere-based Luminex xMAP technology developed in the Vaidya/Bonventre laboratory [14, 15] (**d**). Multiple comparisons were performed with Dunnett's two-tailed test after one-way ANOVA. Data are expressed as means ± SE of 5 rats. $*P < 0.05$, $**P < 0.01$, and $***P < 0.001$, significantly different from the value on day 0.

Figure 4. Immunofluorescence analysis of CCL2 in rats treated with cisplatin. Rats treated with 5 mg/kg cisplatin were used. Kidneys were perfused, fixed with 4% paraformaldehyde, and embedded. The sections (5 µm) were stained with an antibody specific for CCL2 (**red**), phalloidin (**green**), and 4′,6-diamidino-2-phenylindole (DAPI; **blue**). Scale bar, 100 µm. The solid and dotted frames indicate magnifications of the cortex and medullary regions, respectively. Magnification: left panels, ×40; middle and right panels, ×400.

Figure <u>5</u>. Immunofluorescence analysis of Kim-1 in rats treated with cisplatin. Rats

treated with 5 mg/kg cisplatin were used. The kidneys were perfused, fixed with 4%

paraformaldehyde, and embedded. The sections (5 µm) were stained with an antibody

specific for Kim-1 (**red**), phalloidin (**green**), and DAPI (**blue**). Scale bar, 100 µm. The

solid and dotted frames indicate magnifications of the cortex and medullary regions,

respectively. Magnification: left panels, ×40; middle and right panels, ×400.

**Figure <u>6</u>. Immunofluorescence analysis of IL-1beta (a), CCL20 (b), CXCL1 (c), and

CXCL10 (d) in rats treated with cisplatin.** Rats treated with 5 mg/kg cisplatin were used.

The kidneys were perfused, fixed with 4% paraformaldehyde, and embedded. The sections (5

µm) were stained with antibodies specific for IL-1beta, CCL20, CXCL1, or CXCL10. Red

signals for each section were merged with green signals for phalloidin and with blue signals for

DAPI. Scale bar, 100 µm. The solid frame indicates the magnification region. Magnification,

×400.

**Figure <u>7</u>. Measuring urinary and plasma CCL2 and urinary Kim-1 in rats treated with 5

mg/kg cisplatin.** CCL2 concentrations in bladder urine (***open circles***) and plasma (***closed

circles***) in rats given 5 mg/kg cisplatin were measured using enzyme-linked immunosorbent

assay (ELISA) kits (**a**). Kim-1 urinary levels were determined with microsphere-based

Luminex xMAP technology developed in the Vaidya/Bonventre laboratory [14, 15] (**b**).

Concentrations of urinary CCL2 and Kim-1 were normalized to urinary creatinine

concentration. Plasma creatinine (***open circles***) and blood urea nitrogen (***closed circles***) levels

in rats after administration of 5 mg/kg cisplatin are shown (**c**). Multiple comparisons were

performed with Dunnett's 2-tailed test after 1-way ANOVA. Data are expressed as means ±

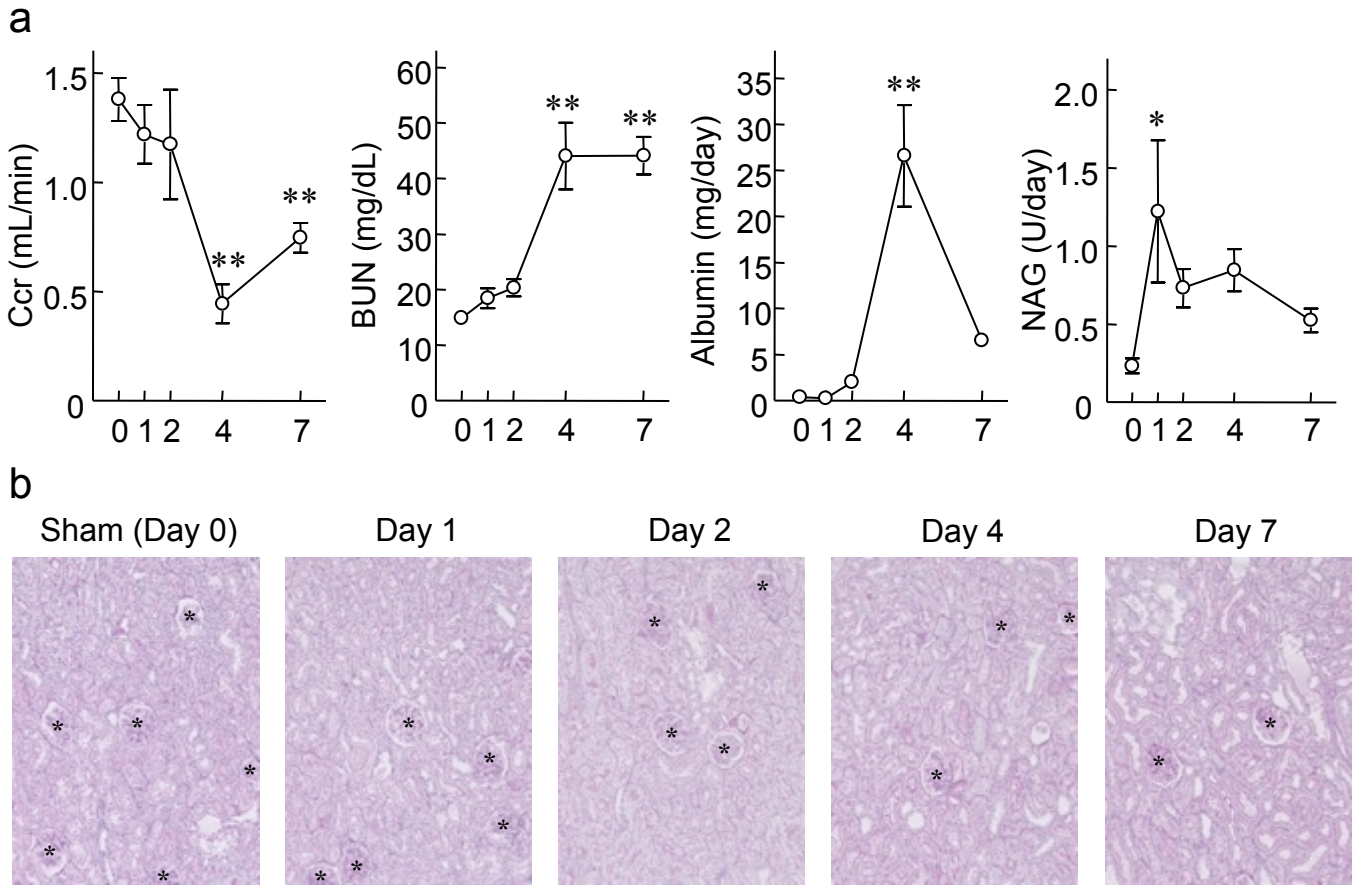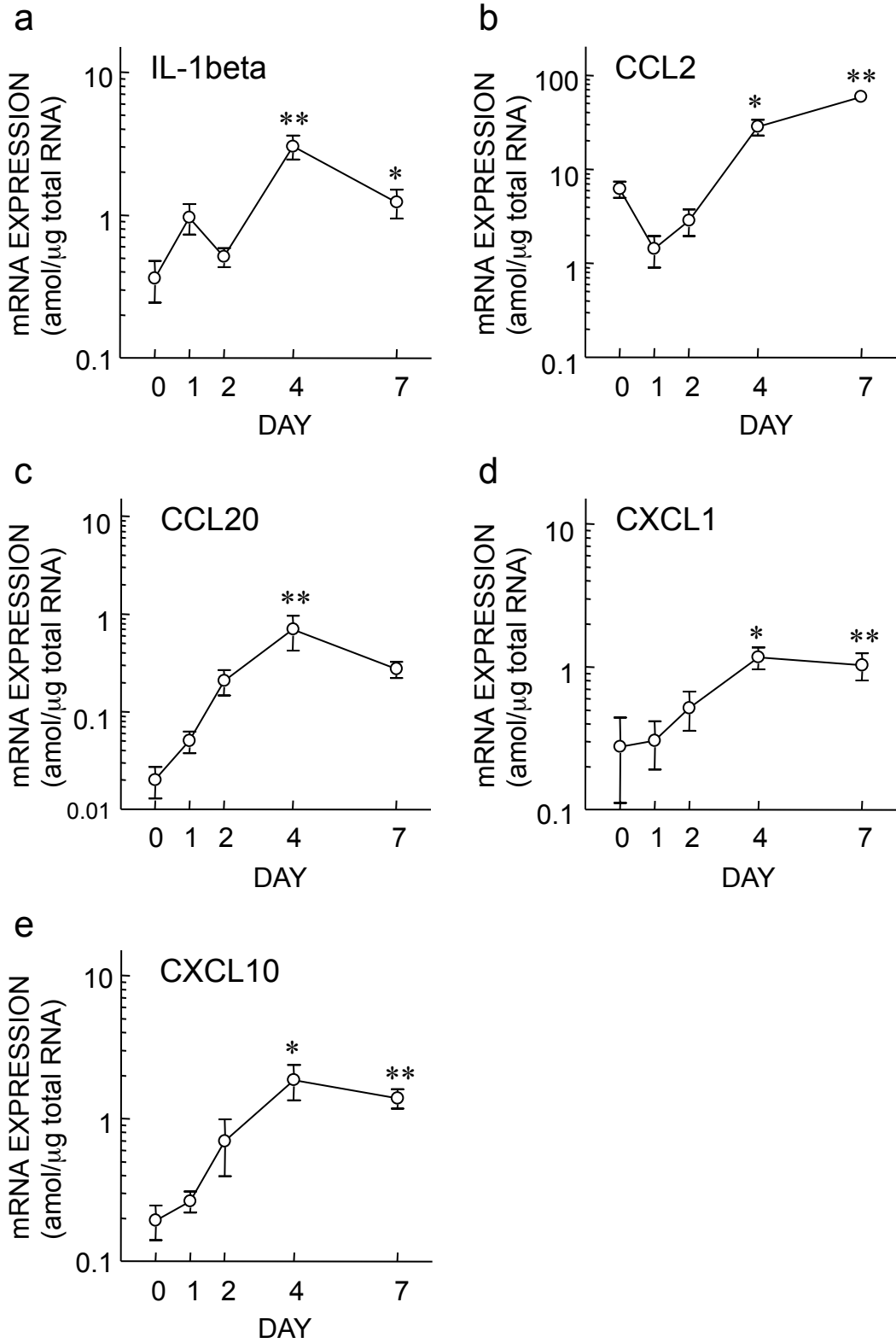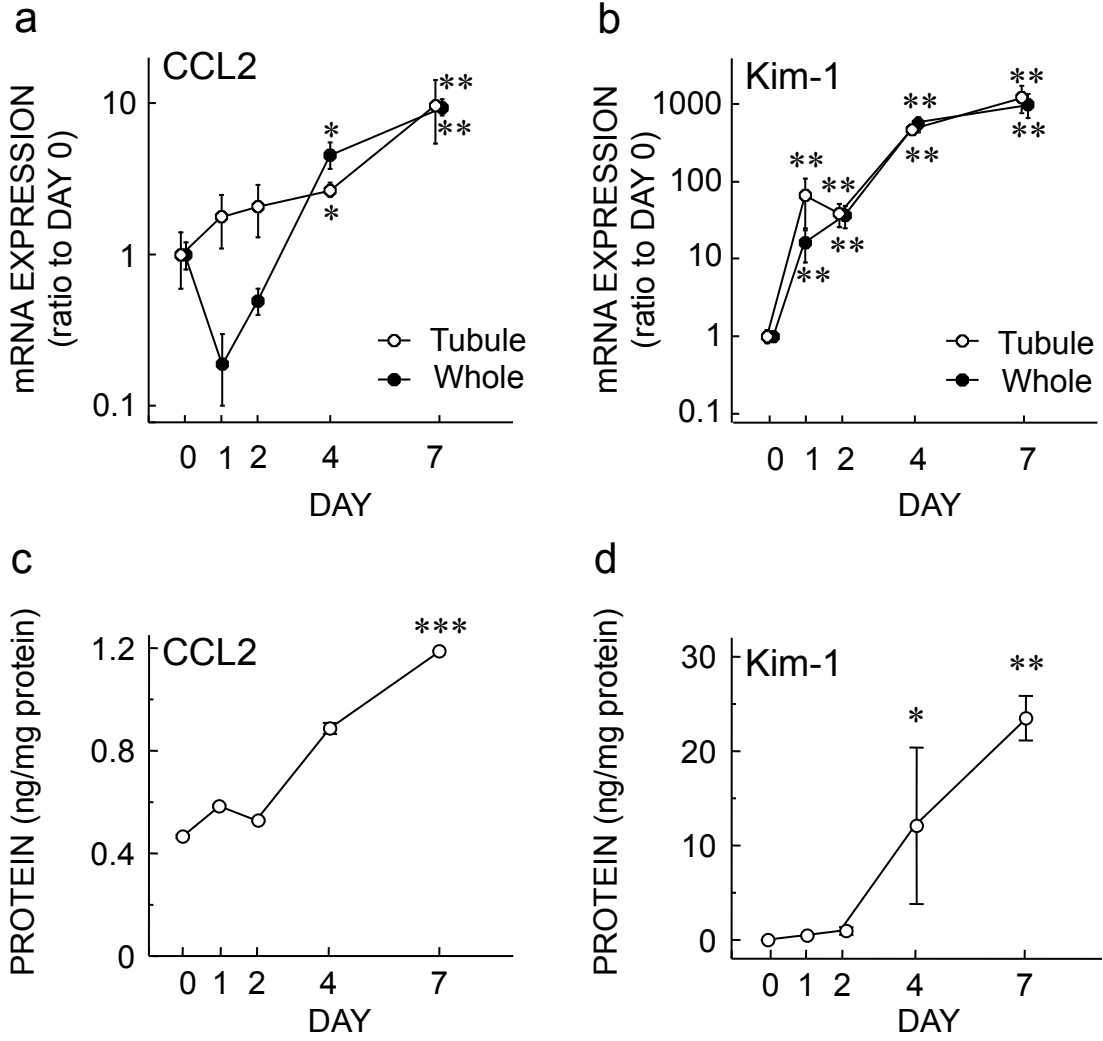S.E. of 5–7 rats. **$P < 0.01$, significantly different from the value on day 0.

Figure <u>8</u>. Measuring urinary and plasma CCL2 and urinary Kim-1 in nephrectomized

rats treated with 2 mg/kg cisplatin. CCL2 concentrations in bladder urine (**a**) or plasma (**b**) in

nephrectomized rats given saline (vehicle, ***open circles***) or 2 mg/kg cisplatin (***closed circles***)

were measured using ELISA kits. Kim-1 urinary levels in nephrectomized rats given saline

(vehicle, ***open circles***) or 2 mg/kg cisplatin (***closed circles***) were determined with

microsphere-based Luminex xMAP technology developed in the Vaidya/Bonventre laboratory

[14, 15] (**c**). Concentrations of urinary CCL2 and <u>KIM</u>-1 were normalized to urinary creatinine

concentration. Plasma creatinine (***open circles***) and blood urea nitrogen levels (***closed circles***)

in nephrectomized rats after administration of corn oil (vehicle, ***open circle***) or 2 mg/kg

cisplatin (***closed circle***) are shown (**d**). Multiple comparisons were performed with Dunnett's

2-tailed test after 1-way ANOVA. Data are expressed as means ± S.E. of 8 rats. **$P < 0.01$,

significantly different from the value on day 0.

Figure 1

a

b

| Sham (Day 0) | Day 1 | Day 2 | Day 4 | Day 7 |

Figure 2

Figure 3

Figure 4

Cortex Medulla

Sham (Day 0) / Day 1 / Day 2 / Day 4 / Day 7

● CCL2 ● phalloidin ● DAPI

Figure 5

Figure 6

a

Sham (Day 0) | Day 1 | Day 2 | Day 4 | Day 7

●IL-1beta　● phalloidin　● DAPI

b

Sham (Day 0) | Day 1 | Day 2 | Day 4 | Day 7

●CCL20　● phalloidin　● DAPI

Figure 6 (Continued)

c

Sham (Day 0) | Day 1 | Day 2 | Day 4 | Day 7

● CXCL1　● phalloidin　● DAPI

d

Sham (Day 0) | Day 1 | Day 2 | Day 4 | Day 7

● CXCL10　● phalloidin　● DAPI

Figure 7

a

b

c

Figure 8